

Synthesis and Aggregation Behavior of *meso*-Sulfinylporphyrins: Evaluation of S-Chirality Effects on the Self-Organization to S–Oxo-Tethered Cofacial Porphyrin Dimers

Yoshihiro Matano,^{*,[a]} Tomonori Shinokura,^[a] Kazuaki Matsumoto,^[a]
Hirosi Imahori,^[a] and Haruyuki Nakano^[b]

In memory of Professor Yoshihiko Ito

Abstract: The synthesis and aggregation behavior of *meso*-sulfinylporphyrins are described. The copper-catalyzed C–S cross-coupling reaction of a *meso*-iodoporphyrin with benzenethiol and *n*-octanethiol has proved to be an efficient method for the synthesis of *meso*-sulfinylporphyrins, which are oxygenated by *m*-chloroperbenzoic acid to produce the corresponding *meso*-sulfinylporphyrins. Optically active zinc *meso*-sulfinylporphyrins were successfully isolated by means of optical resolution of the racemates on a chiral HPLC column. Zinc sulfinylporphyrins readily undergo self-organization through S–oxo–zinc coordination to form cofacial porphyrin dimers in solution, in which the hetero- and

homodimers are present as a diastereomeric mixture. The aggregation modes of the S–oxo-tethered porphyrin dimers were fully characterized by ¹H NMR, IR, and UV/Vis spectroscopy as well as DFT calculations on their model compounds, thus revealing that the self-aggregation behavior depends on the combination of S chirality. The absolute configurations at the sulfur center can be determined by the exciton-coupled CD method. The observed self-association constant for the S–oxo-tethered dimerization of (*S*)-phenylsul-

finylporphyrin in toluene is larger than that in dichloromethane, which reflects the difference in dipole moments between the homodimer and the monomer. In cyclic and differential pulse voltammetry, the first oxidation process of the cofacial dimers is split into two reversible steps, which indicates that the initially produced π radical cations are delocalized efficiently between the two porphyrin rings. The present findings demonstrate the potential utility of *meso*-sulfinyl groups as promising ligands for investigating the effects of peripheral chirality on the structures and optical and electrochemical properties of metal-assisted porphyrin self-assemblies.

Keywords: chirality • cross-coupling • porphyrinoids • self-assembly • S–O compounds

Introduction

In natural photosynthetic reaction centers, porphyrin pigments are arranged in well-defined structures, which are indispensable for exhibiting high efficiencies in their light-harvesting abilities and their energy- and electron-transfer processes.^[1] To understand the role of the specific arrangement of the chromophores, a number of artificial reaction-center models, which consist of covalently or noncovalently linked multiporphyrin arrays, have been provided. Among them, metal-to-ligand coordinative interaction has been frequently used to connect and organize metalloporphyrin pigments, as the three-dimensional geometries and distances of the chromophores can be controlled by changing the combination of central metals and peripherally substituted ligands.^[2] Such structural diversity is also beneficial for the design of new

[a] Prof. Y. Matano, T. Shinokura, K. Matsumoto, Prof. H. Imahori
Department of Molecular Engineering
Graduate School of Engineering
Kyoto University, Nishikyo-ku
Kyoto 615-8510 (Japan)
Fax: (+81) 75-383-2571
E-mail: matano@scl.kyoto-u.ac.jp

[b] Prof. H. Nakano
Department of Chemistry
Graduate School of Sciences
Kyushu University
Fukuoka 812-8581 (Japan)

Supporting information for this article is available on the WWW under <http://www.chemasianj.org> or from the author.

classes of supramolecular porphyrin-based materials. For effective electronic communication between the organized porphyrin π systems, it is desirable to attach coordination sites directly to or near the peripheral (*meso* or β) positions of the porphyrin ring. In this respect, various N and O bases such as pyridyl,^[3] imidazolyl,^[4] amine,^[5] and hydroxy/carbonyl^[6] groups have been examined as peripherally substituted ligands to construct cofacial, linear, branched, cyclic, dendritic, and polymeric metalloporphyrin self-assemblies. In these systems, the directional angle and basicity of the lone-pair electrons of the ligands define the geometries, stabilities, and optical and electrochemical properties of the assemblies. However, other classes of peripheral ligands, especially those that bear chirality at the coordination sites, have not yet been fully explored.

The supramolecular chemistry of organized chiral porphyrins has also received increasing attention because of their utility as receptors for sensing chiral molecules and as chiral models for investigating the photophysical and electrochemical events that occur at natural reaction centers.^[7] Chiral spacers derived from amino acids, sugars, and other chiral sources with carbon-centered chirality have been frequently used to construct asymmetrically organized multiporphyrin arrays. In contrast, little attention has been paid to heteroatom-centered chirality in metal-assisted porphyrin self-assemblies.

Recently, Arnold and co-workers^[8] and our group^[9] independently reported the first examples of *meso*-phosphorylporphyrins, which bear a polarized P–oxo bond at the *meso* position. It was clarified that the *meso*-phosphorylporphyrin metal complexes readily undergo self-organization through P–oxo–metal (Zn or Mg) coordination to form cofacial dimers in solution and in the solid state or zig-zag polymers in the solid state. It is of particular interest that the P–oxo-tethered cofacial dimers exhibit characteristic electrochemical properties owing to the electronic communication between the two partially stacked porphyrin π systems. In other words, the P–oxo-tethered zinc porphyrin dimers showed 1e/1e/2e electrochemical oxidation processes,^[9] which was not previously observed for tightly stacked 2-pyridyl- and 2-imidazolyl-tethered zinc porphyrin dimers.^[3f,4f] These findings represent the potential utility of third-row heteroatom–oxo substituents as moderately basic coordination sites for metalloporphyrin self-assemblies. Therefore,

we turned our attention to sulfinyl groups, which contain both a polarized sulfur–oxo bond and stable chirality at the sulfur center. The latter feature seems highly promising for investigating the influence of peripheral chiral auxiliaries on the geometries and fundamental properties of metal-assisted porphyrin self-assemblies.

In 1991, Crossley and co-workers reported a β -phenylsulfinylporphyrin in their systematic study on β -substituent effects on the frontier orbitals of 5,10,15,20-tetraphenylporphyrin metal complexes.^[10] To the best of our knowledge, however, there are no examples of *meso*-sulfinylporphyrins and their chiral derivatives, probably due to the lack of a general method for the preparation of this class of compounds. It is widely known that peripheral carbon–heteroatom bonds are conveniently formed by palladium-catalyzed cross-coupling reactions between haloporphyrins and the corresponding heteroatom reagents. For instance, porphyrins that bear boron-,^[11] oxygen-,^[12] nitrogen-,^[13] phosphorus-,^[8,9] and sulfur-derived^[14] functional groups at the *meso* or β positions have been prepared by this methodology. Ligand-free nickel-catalyzed C–O and C–N cross-coupling reactions have also been used for attaching phenoxy and amine functionalities.^[15] Recently, we found that the copper-catalyzed C–P cross-coupling reaction between a *meso*-iodoporphyrin and organophosphorus(V) reagents is applicable to the synthesis of *meso*-phosphorylporphyrins.^[9] With this result in hand, we decided to use the copper-catalyzed C–S cross-coupling reaction as a key step for the synthesis of *meso*-sulfinylporphyrins.

Herein, we report the first examples of *meso*-sulfinylporphyrins. Zinc sulfinylporphyrins were found to undergo self-organization in nonpolar and moderately polar solvents to form cofacial dimers through S–oxo–zinc complementary coordination. We also succeeded in isolating optically active zinc sulfinylporphyrins and revealed the effects of S chirality on self-aggregation behavior. The observed optical and electrochemical properties of cofacial zinc sulfinylporphyrin dimers exemplify the potential utility of the peripheral sulfinyl ligands for the construction of metal-assisted chiral porphyrin self-assemblies.

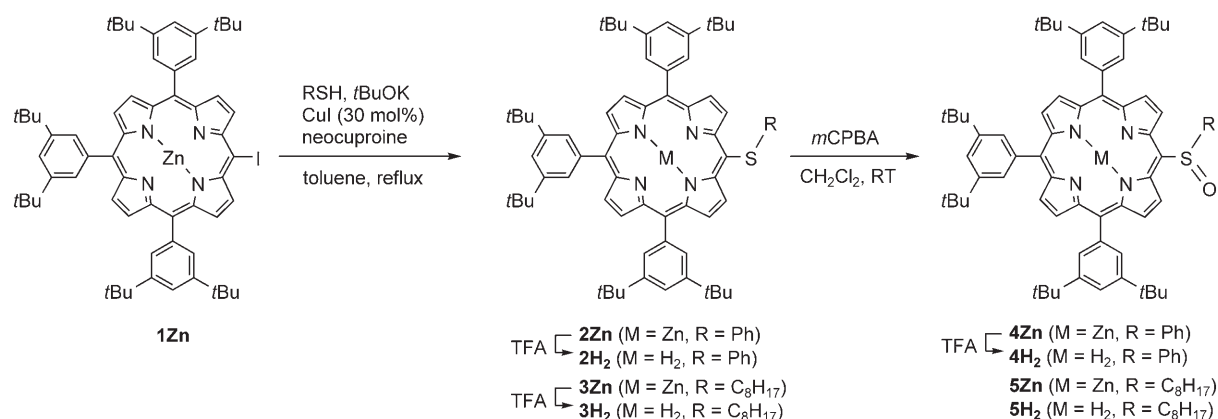
Results and Discussion

Synthesis of *meso*-Sulfinylporphyrins

The synthesis of *meso*-sulfinylporphyrins is summarized in Scheme 1. The copper-catalyzed C–S cross-coupling reaction of *meso*-iodoporphyrinatozinc(II) **1Zn**^[16] with benzenethiol and *n*-octanethiol under the Venkataraman conditions^[17] afforded the corresponding *meso*-sulfanylporphyrins **2Zn** and **3Zn** in 94 and 80% yield, respectively. The present method is as efficient as the palladium-catalyzed C–S cross-coupling reaction reported by Zhang and co-workers^[14] and the S_NAr reaction of 5-nitrooctaethylporphyrins with benzenethiolate reported by Crossley et al.^[18] Treatment of **2Zn** and **3Zn** with 1 equivalent of *m*CPBA in CH_2Cl_2 gave *meso*-sulfinylporphyrins **4Zn** and **5Zn** in 62 and 80% yield, respectively.

Abstract in Japanese:

銅触媒を用いた炭素-硫黄クロスカップリング反応を経由してメソスルフィニルポルフィリンを合成し、その光学活性体を単離した。亜鉛スルフィニルポルフィリンは、非極性溶媒中、スルフィニル酸素から亜鉛への配位を利用した相補的な二量体を形成し、ヘテロ/ホモ二量体の混合物として存在することを、各種スペクトルおよびDFT計算により明らかにした。さらに、二量体の可視紫外吸収スペクトルおよび電気化学測定を行い、相補的な会合形態が亜鉛スルフィニルポルフィリンの吸収特性や電気化学的酸化過程に大きな影響を与えることを見いだした。



Scheme 1. Synthesis of *meso*-sulfinylporphyrins. *m*CPBA = *m*-chloroperbenzoic acid, TFA = trifluoroacetic acid.

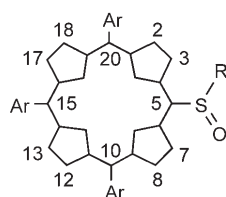
Demetalation of zinc porphyrins **2Zn**, **3Zn**, and **4Zn** with TFA in CH₂Cl₂ yielded the corresponding free bases **2H₂**, **3H₂**, and **4H₂**. Compounds **4H₂** and **5H₂** can be alternatively prepared by selective oxidation of **2H₂** and **3H₂** with *m*CPBA.

Characterization and Aggregation Behavior of *meso*-Sulfinylporphyrins

The structures of newly synthesized porphyrins **2M–5M** (M = Zn, H₂) were characterized by means of ¹H NMR, UV/Vis, and IR spectroscopy as well as mass spectrometry. In the ¹H NMR spectra of *meso*-sulfinylporphyrins **2M** and **3M** in CDCl₃, all proton signals were observed as sharp peaks at normal regions for AB₃-type *meso*-tetrasubstituted porphyrins (see Supporting Information, Figures S1–S4). The *meso*-sulfinylporphyrin free bases **4H₂** and **5H₂** also showed distinct peaks, in which the peripheral 3,7-β (**4H₂** and **5H₂**), S-phenyl *ortho* (**4H₂**), and S-methylene (**5H₂**) proton signals were observed at δ = 9.98 (**4H₂**) and 10.18 (**5H₂**), 7.64, and 3.55–4.06 ppm, respectively (see Supporting Information, Figures S5 and S6; for the numbering scheme, see Scheme 2). Oxygenation at the sulfur atom (from **2H₂**, **3H₂** to **4H₂**, **5H₂**) induced slight downfield shifts in the signals of the 3,7-β protons (Δδ = 0.12–0.20 ppm). The diastereotopic appearance of the S-methylene proton signals of **5H₂** represents stable chirality at the sulfur center. The S chirality of **4H₂** and **5H₂** does not discriminate the 3,7-β protons clearly at 25 °C, which suggests that the *meso*-carbon–sulfur bond rotates rapidly on the NMR timescale at room temperature.

However, the signals for these protons were observed diastereotopically at low temperatures.^[19]

The ¹H NMR spectra of zinc *meso*-sulfinylporphyrins **4Zn** and **5Zn** in CD₂Cl₂ showed complicated peak patterns derived from two different species (Figures 1b and 2b). Thus, all



Scheme 2. Numbering scheme of the sulfinylporphyrins.

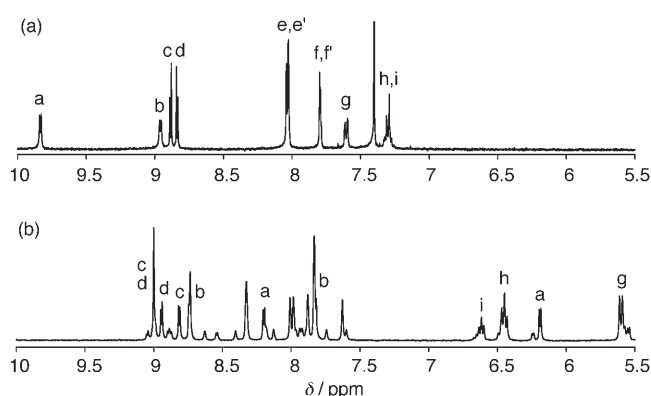


Figure 1. ¹H NMR spectra of **4Zn** (δ = 5.5–10.0 ppm). a = 3,7-β, b = 2,8-β, c = 12,18-β, d = 13,17-β, e = 10,20-*meso*-aryl H_o, e' = 15-*meso*-aryl H_o, f = 10,20-*meso*-aryl H_p, f' = 15-*meso*-aryl H_p, g = S-phenyl H_o, h = S-phenyl H_m, i = S-phenyl H_p. For the labeling, see Scheme 2. a) Recorded in CDCl₃/CD₃OD (5:1 v/v, 1.6 × 10⁻³ M) at 25 °C. b) Recorded in CD₂Cl₂ (1.6 × 10⁻³ M) at –10 °C. Labeled peaks are those derived from the major diastereomer (heterodimer).

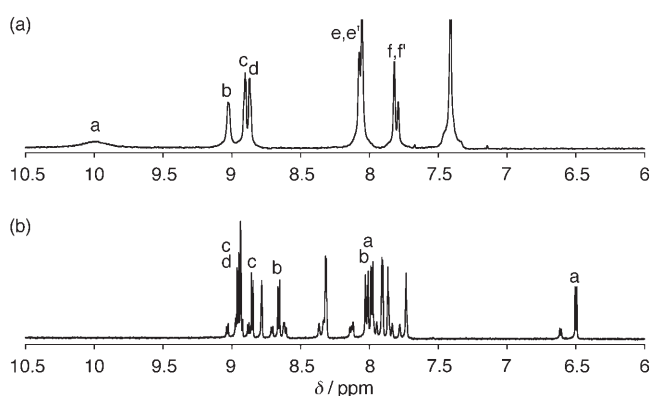


Figure 2. ¹H NMR spectra of **5Zn** (δ = 6.0–10.5 ppm). a = 3,7-β, b = 2,8-β, c = 12,18-β, d = 13,17-β, e = 10,20-*meso*-aryl H_o, e' = 15-*meso*-aryl H_o, f = 10,20-*meso*-aryl H_p, f' = 15-*meso*-aryl H_p. For the labeling, see Scheme 2. a) Recorded in CDCl₃/CD₃OD (5:2 v/v, 1.6 × 10⁻³ M) at 25 °C. b) Recorded in CD₂Cl₂ (2.0 × 10⁻³ M) at 25 °C. Labeled peaks are those derived from the major diastereomer (heterodimer).

the β protons of **4Zn** and **5Zn** appear to be nonequivalent, which indicates the magnetically unsymmetrical environments for the porphyrin rings in each species.^[20] The separately observed peaks of the major and minor species of **4Zn** and **5Zn** were assigned by means of ^1H - ^1H COSY measurements. The most diagnostic feature of their ^1H NMR spectra is the upfield appearance of the signals of the 3,7- β , S-phenyl (**4Zn**), and S-methylene (**5Zn**) protons relative to the corresponding signals for **4H₂** and **5H₂**. Such magnetic shielding is apparently due to the ring-current effect of the neighboring porphyrin π electrons. It is therefore likely that the zinc sulfinylporphyrins exist as two types of self-aggregates through metal-ligand coordination. In fact, the UV/Vis spectra of **4Zn** and **5Zn** showed concentration dependence (see below), whereas those of **4H₂** and **5H₂** did not.

On the other hand, the ^1H NMR spectra of **4Zn** and **5Zn** in $\text{CDCl}_3/\text{CD}_3\text{OD}$ (5:1–5:2 *v/v*) displayed completely different peak patterns derived from single species, in which all peaks appeared in the same regions as those of **4H₂** and **5H₂** (Figures 1a and 2a; see also Supporting Information, Figures S7 and S8). For instance, the 3,7- β , S-phenyl *ortho* (**4Zn**), and S-methylene (**5Zn**) protons were observed at $\delta = 9.83$ (**4Zn**) and 9.88 (**5Zn**), 7.61, and 3.65–4.04 ppm, respectively. Addition of an excess amount of pyridine into the solutions of **4Zn** and **5Zn** in CDCl_3 also changed the peak appearances dramatically, such that distinct peaks due to the pyridine adducts **4Zn-py** and **5Zn-py** were displayed (see Experimental Section for measurement conditions). These results suggest that methanol and pyridine coordinate to the zinc centers of **4Zn** and **5Zn** to cause dissociation of the aggregates to the respective zinc sulfinylporphyrin monomers. Methanol may also act as a hydrogen-bond donor for the polarized S-oxo group. The effects of these additives on the ^1H NMR spectra resemble those observed for zinc phosphorylporphyrins, which exist as P-oxo-tethered cofacial dimers in nonpolar and moderately polar solvents.^[9]

In the IR spectra of solid samples prepared as Nujol mulls, strong S=O stretching bands of **4Zn** ($\tilde{\nu} = 992$ – 1006 cm^{-1}) were observed at lower frequencies than that of **4Zn-py** ($\tilde{\nu} = 1037\text{ cm}^{-1}$), which indicates that the multiple-bond character of the S-oxo bond is considerably weakened by self-aggregation (see Supporting Information, Figure S9). It is known that O-bound metal-sulfoxide complexes exhibit S=O stretching vibration bands at lower frequencies than free sulfoxides.^[21] In this regard, the sulfinyl group in **4Zn** is considered to coordinate to the zinc center via an oxygen atom. This agrees well with the fact that sulfanylporphyrins **2Zn** and **3Zn** and free-base sulfinylporphyrins **4H₂** and **5H₂** do not form self-aggregates.

We note again that the sulfinyl groups of **4Zn** and **5Zn** contain stable chirality at the sulfur center. To discuss the effect of S chirality on the self-organization of zinc sulfinylporphyrins, we attempted to separate the two enantiomers of **4Zn** and **5Zn** by using a semipreparative, chiral carbamate-modified polysaccharide HPLC column. The chromatographic conditions are described in the caption of Figure 3.

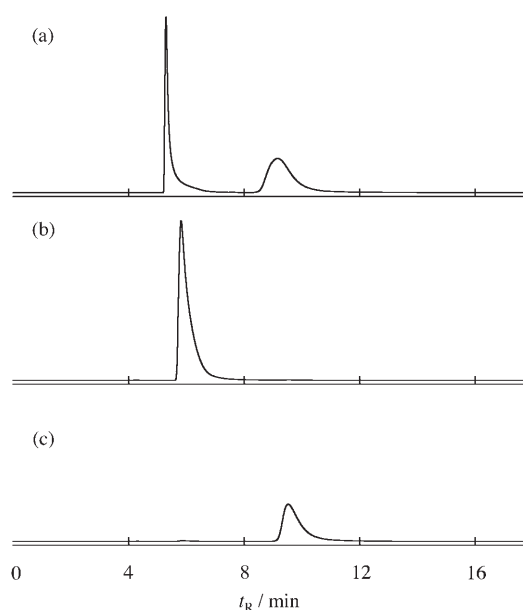


Figure 3. HPLC chromatograms of **4Zn**. DAICEL Chiralpak IA, hexane/2-propanol (100:1), 1.0 mL min^{-1} at 25°C , monitored at 425 nm. a) The racemate (before separation). b) The first fraction (after separation). c) The second fraction (after separation).

As shown in Figure 3, both enantiomers of the phenylsulfinylporphyrin **4Zn** were isolated in high optical purities (99% *ee* for the 1st fraction, 97% *ee* for the 2nd fraction). On the other hand, the octylsulfinylporphyrin **5Zn** could not be resolved completely under the same conditions (79% *ee* for the 1st fraction, 50% *ee* for the 2nd fraction); the reason for that is not clear.

With optically active zinc sulfinylporphyrins in hand, the structures of zinc sulfinylporphyrin aggregates can now be discussed in more detail. In the ^1H NMR spectra of the racemates of **4Zn** and **5Zn** in CD_2Cl_2 (Figures 1b and 2b), two sets of peaks were observed, which indicates that a pair of diastereomers was present in solution. Unfortunately, attempts to measure the molecular weights of the **4Zn** and **5Zn** aggregates in solution by vapor-pressure osmometry were unsuccessful due to their limited solubility. However, the ESI mass spectra of **4Zn** and **5Zn** in $\text{CHCl}_3/\text{CH}_3\text{CN}$ showed parent-ion peaks at $m/z = 2148$ and 2220, respectively, which are attributed to dimeric cations ($[2M + \text{Na}]^+$; see Supporting Information, Figure S10). Hence, the zinc sulfinylporphyrin aggregates are considered to be present mostly as a diastereomeric mixture of the S-oxo-tethered dimers in nonpolar and moderately polar solvents.^[22]

When the ^1H NMR spectrum of optically pure **4Zn** (1st fraction, 99% *ee*) was recorded in CD_2Cl_2 , only one set of peaks corresponding to the minor diastereomer appeared (Figure 4b and d). By comparison with the ^1H NMR spectrum of the **4Zn** racemate (Figure 4a and c), we can safely conclude that the major and minor diastereomers observed for the racemates are the *S,R* heterodimer and the *S,S/R,R* homodimers, respectively. In the spectrum of the optically pure **4Zn** homodimer at -40°C (Figure 4d), the peaks at

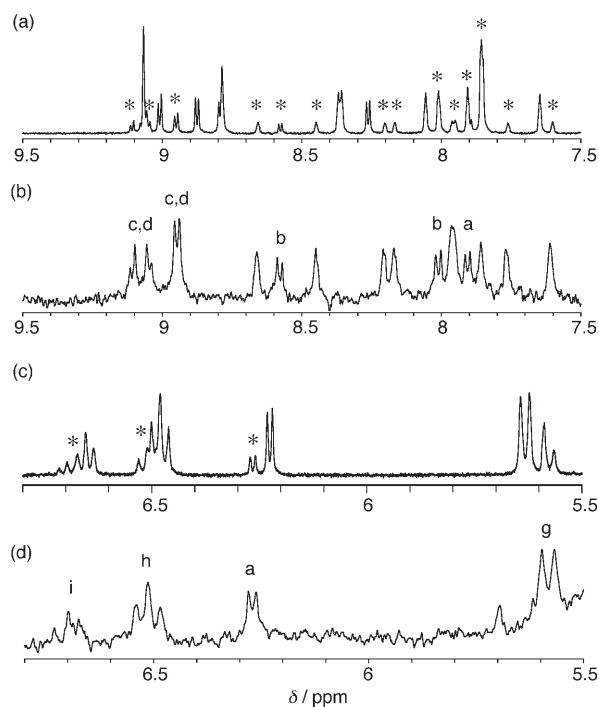


Figure 4. ^1H NMR spectra of **4Zn** in CD_2Cl_2 at -40°C a) and b) from $\delta = 5.5$ to 6.8 ppm and c) and d) from $\delta = 7.5$ to 9.5 ppm. a) and c) The racemate (1.6×10^{-3} M). Asterisks indicate selected peaks from the minor diastereomer (homodimer). b) and d) The *S* isomer (5×10^{-4} M). All peaks are from the *S,S* homodimer: a = 3,7- β , b = 2,8- β , c = 12,18- β , d = 13,17- β , g = S-phenyl H_o , h = S-phenyl H_m , i = S-phenyl H_p . For the labeling, see Scheme 2.

$\delta = 5.58$, 6.51 , and 6.70 ppm were assigned to the S-phenyl *ortho*, *meta*, and *para* protons on the basis of their coupling patterns and integral values (Table 1). The signals of the S-phenyl protons of the **4Zn** heterodimer were also observed at $\delta = 5.60$ – 6.62 ppm. The large upfield shifts of the signals of the S-phenyl protons of the dimers relative to those of the monomer (Figure 1 a) resulted from the ring-current effect of the porphyrin π circuit, which suggests that the S-phenyl group is located above the second porphyrin ring in the dimeric state. The degree of shielding decreases in the order *ortho* ($\Delta\delta = 2.01$ – 2.03 ppm) > *meta* ($\Delta\delta = 0.79$ – 0.85 ppm) > *para* ($\Delta\delta = 0.60$ – 0.68 ppm). Although the signal-to-noise (S/N) ratio of the ^1H NMR spectrum of optically active **5Zn** (1st fraction, 79% *ee*) was low, the major and

minor diastereomers could also be assigned as the hetero- and homodimers, respectively. The S-methylene protons of the **5Zn** homo- and heterodimers are more shielded ($\Delta\delta = 1.69$ – 1.82 ppm) than those of the **5Zn** monomer. These data strongly support the hypothesis that zinc sulfinylporphyrins exist as a diastereomeric mixture of complementary S-oxo-tethered cofacial dimers in weakly polar solvents. The fact that signals for both homo- and heterodimers were observed separately in the ^1H NMR spectra implies that the interconversion between the two diastereomers of the zinc sulfinylporphyrins is slow on the NMR timescale.

The hetero-/homodimer ratios of the **4Zn** and **5Zn** dimers in CD_2Cl_2 were found to be 4.7:1 and 4:1, respectively, on the basis of signal integration of the ^1H NMR spectra (2.0×10^{-3} M, -10°C). Thus, the heterodimer is thermodynamically more stable than the homodimer, although the differences in the ground-state energies between the two are very small (3.0 – 3.4 kJ mol $^{-1}$ at -10°C). In the observed temperature range (-10 to -50°C), the hetero-/homodimer ratio did not vary within experimental error, which suggests that the temperature dependence of the self-association constants of the hetero- and homodimers are similar.

To gain further insight into the structures of S-oxo-tethered zinc sulfinylporphyrin dimers, density functional theory (DFT) calculations at the B3LYP/6-31G(d,p) level were carried out on 5-phenylsulfinyl-10,15,20-triphenylporphyrinato-zinc(II) (**6**) as a model for **4Zn**. The optimized structures of the *S,R* heterodimer, the *S,S* homodimer, and the *S* monomer of **6** are depicted in Figure 5. Selected bond lengths, interatomic distances, bond angles, and dihedral angles are listed in Table 2. Scheme 3 shows schematic views of the cofacial dimers of the zinc sulfinylporphyrins. The sulfur center in each dimer adopts trigonal-pyramidal geometry with a sum of C–S–X (X = C, O) bond angles of 315.9 – 316.2° , which is close to that ($\Sigma_{\text{C-S-X}} = 316.0^\circ$) of the monomer. As a result of the S-oxo–Zn coordinative interaction, the O–S–C_{meso}–C $_{\alpha}$ dihedral angles (41.2 – 42.2°) of the dimers are widened compared to the respective angle of the monomer (37.5°). Furthermore, the five-coordinate zinc atom is displaced from the mean plane formed by the four nitrogen atoms (0.415 Å for the homodimer, 0.409 Å for the heterodimer), and the porphyrin rings are slightly distorted. The S–O bonds (1.551 – 1.552 Å) of the dimers are appreciably longer than that (1.517 Å) of the monomer, which indicates that the double-bond character of the S-oxo bond is decreased by dimerization, as deduced from the IR spectra.

The Zn–O distances and S–O bond lengths of the homodimer are close to the respective values of the heterodimer, which suggests that there is little difference in the degree of S-oxo–zinc coordinative interaction between the homo- and heterodimers. However, the whole geometry of the hetero-

Table 1. Selected ^1H NMR chemical shifts (ppm) for **4Zn** and **5Zn**.^[a]

Proton	4Zn			5Zn		
	Monomer ^[b]	Heterodimer ^[c]	Homodimer ^[c]	Monomer ^[d]	Heterodimer ^[e]	Homodimer ^[e]
3,7- β	9.83	6.19, 8.20	6.27, 7.91	9.88	6.50, 7.98	6.61, 7.73
2,8- β	8.96	7.82, 8.74	8.01, 8.58	9.00	7.98, 8.66	8.14, 8.71
S-Ph <i>ortho</i>	7.61	5.60	5.58	–	–	–
S-Ph <i>meta</i>	7.30	6.45	6.51	–	–	–
S-Ph <i>para</i>	7.30	6.62	6.70	–	–	–
S-CH ₂	–	–	–	3.65, 4.04	1.96, 2.22	1.96, 2.32

[a] Relative to tetramethylsilane (TMS). [b] Recorded in $\text{CDCl}_3/\text{CD}_3\text{OD}$ (5:1 v/v) at 25°C . [c] Recorded in CD_2Cl_2 at -10°C . [d] Recorded in $\text{CDCl}_3/\text{CD}_3\text{OD}$ (5:2 v/v) at 25°C . [e] Recorded in CD_2Cl_2 at 25°C .

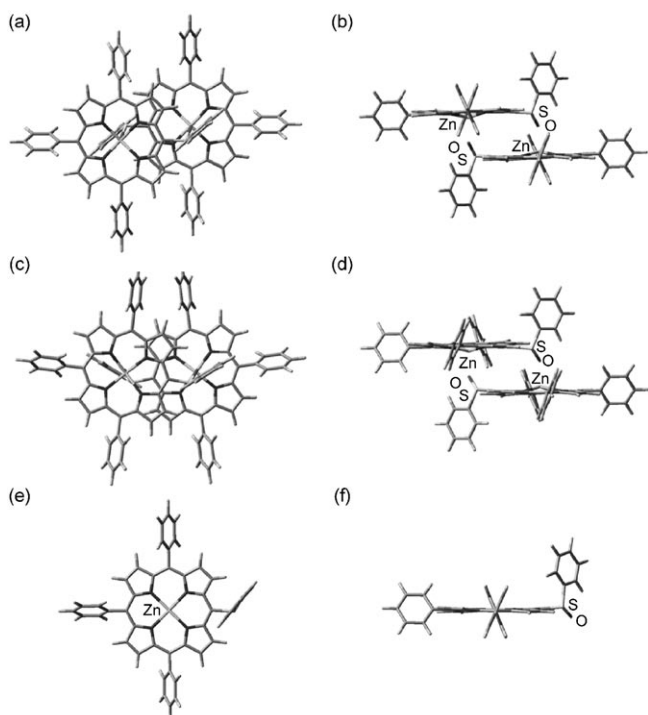


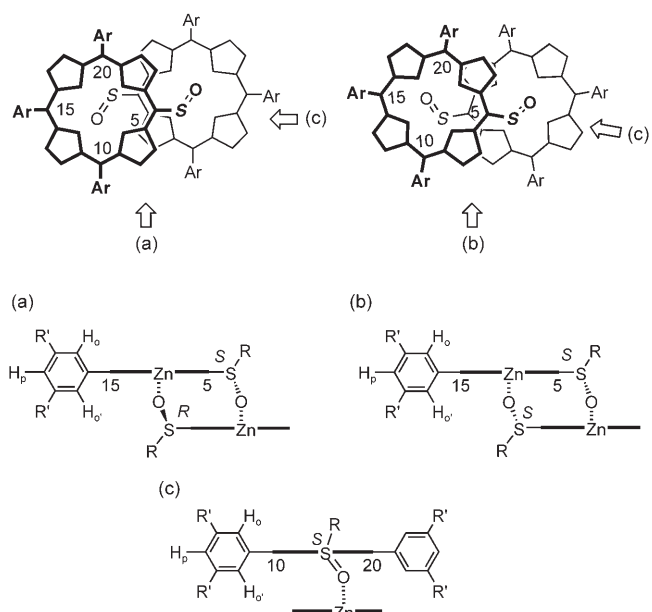
Figure 5. Top and side views of the optimized structures of a) and b) the *S,R* heterodimer, c) and d) the *S,S* homodimer, and e) and f) the *S* monomer of **6**.

Table 2. Selected calculated structural parameters of **6**.

	Heterodimer	Homodimer	Monomer
Zn–O [Å]	2.109	2.112	–
S–O [Å]	1.551	1.552	1.517
Zn···Zn [Å]	6.488	6.502	–
O–S–C _{meso} [°]	110.2	110.1	111.6
O–S–C _{Ph} [°]	103.1	103.3	106.2
O–S–C [°]	102.6	102.8	98.2
Zn–O–S [°]	128.3	126.5	–
O–S–C _{meso} –C _α [°]	41.2	42.2	37.5

dimer clearly differs from that of the homodimer; the two porphyrin rings of the former are linked in a parallel manner with C_i symmetry, whereas those of the latter are linked helically with C_2 symmetry.

The optimized structures of the **6** dimers reasonably explain the upfield appearances of the signals of the S–phenyl and peripheral 3,7-β protons of the **4Zn** dimers in their ¹H NMR spectra (Table 1). As illustrated in Figure 5, these protons are located above the porphyrin ring of the counterpart. The aggregation modes in Scheme 3 also support non-equivalence of the β protons and the inner and outer aryl protons of the *meso*-3,5-di-*tert*-butylphenyl groups of **4Zn**, which are discriminated in the dimeric state.^[23] The Zn···Zn separations of 6.488–6.502 Å calculated for the **6** dimers are somewhat longer than that (6.25 Å) of the structurally characterized, cofacial zinc *meso*-dibutoxyphosphorylporphyrin dimer, which has C_{2h} symmetry in the solid state and in solution. By taking the structural parameters of **6** into consider-



Scheme 3. Schematic views of the zinc sulfanylporphyrin *S,R* hetero- and *S,S* homodimers. **4Zn**: Ar = 3,5-di-*tert*-butylphenyl (R' = *t*Bu), R = Ph; **5Zn**: Ar = 3,5-di-*tert*-butylphenyl (R' = *t*Bu), R = *n*-C₈H₁₇; **6**: Ar = Ph (R' = H), R = Ph. a) and b) Side views along the 10–20 axis. c) Side view along the 5–15 axis.

ation, zinc *meso*-sulfanylporphyrins may be regarded as new chiral models for a weakly coupled chlorophyll pair in the photosynthetic reaction center.^[24]

The isolation of optically active zinc sulfanylporphyrins **4Zn** and **5Zn** led us to determine the absolute configuration at the sulfur center by using the exciton-coupled CD method.^[25] The CD spectra of the separated enantiomers of **4Zn** were recorded in toluene at 1.0×10^{-4} M. Under these conditions, the homodimer and the monomer are considered to be present in a 4:1 ratio (see below). As shown in Figure 6, large Cotton effects were observed for the two fractions with opposite signs: the first fraction showed a positive-to-negative pattern on going from longer to shorter wavelengths, whereas the second fraction showed a negative-to-positive pattern. By contrast, in the presence of excess MeOH, the CD spectrum of **4Zn** (the first fraction) showed much weaker Cotton effects derived from the optically active monomer. These observations strongly support the helical array of the porphyrin chromophores in the S-oxo-tethered homodimer, as illustrated in Scheme 3. The optically active zinc sulfanylporphyrin **5Zn** also showed large Cotton effects with the same CD couplets as those observed for the optically active **4Zn** (see Supporting Information, Figure S11).

The intense Soret bands of porphyrins are a reliable tool for the exciton-coupled CD method, because the signs and amplitudes of the CD curves are related to the absolute helicity of the electronic-transition moments of the chromophores. In fact, optically active porphyrin aggregates covalently or noncovalently linked by chiral spacers have been reported to exhibit large Cotton effects in their CD spec-

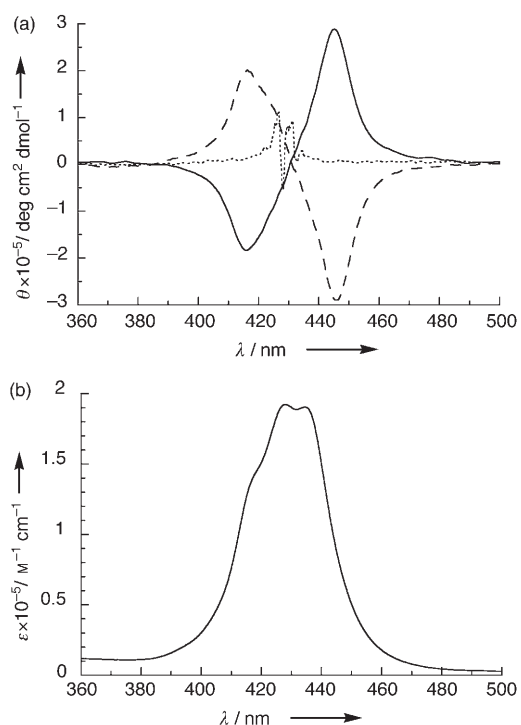
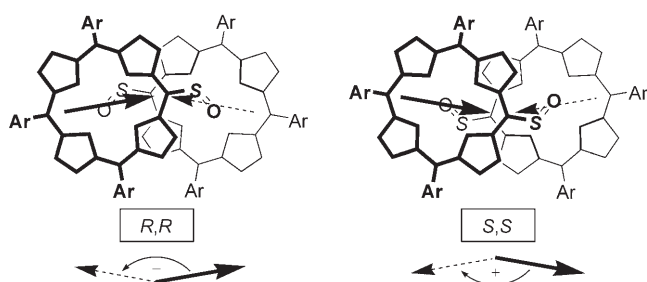


Figure 6. a) CD spectra of the optically active **4Zn** in toluene at 1.0×10^{-4} M. The first and second fractions are shown as solid and dashed lines, respectively. Dotted line: the first fraction in the presence of 10% MeOH. b) UV/Vis spectrum of (*S*)-**4Zn** in toluene at 1.0×10^{-4} M.

tra.^[7] As the zinc sulfinylporphyrin **4Zn** is likely to have a dipole moment along the 5–15 axis, the positive CD couplet observed for the first fraction is indicative of a positive dihedral angle between the porphyrin chromophores of the homodimer (Scheme 4). Accordingly, the absolute configuration of the sulfur center of the enantiomerically pure **4Zn** obtained from the first fraction was assigned as *S*, and that obtained from the second fraction as *R*.



Scheme 4. Assignment of the chirality of the zinc sulfinylporphyrins.

Optical Properties of meso-Sulfinylporphyrins

As discussed above, zinc sulfinylporphyrins **4Zn** and **5Zn** undergo self-organization to give the *S*-oxo-tethered cofacial dimers in weakly polar solvents. To reveal the dimerization effect on the optical properties of zinc sulfinylporphyrins, we first recorded the UV/Vis spectra of enantiomerically

pure (*S*)-**4Zn** (>99% *ee*) in toluene at 2.0×10^{-7} – 1.0×10^{-4} M. As shown in Figure 7, the monomer Soret band was split by dimerization at higher concentrations, and the exci-

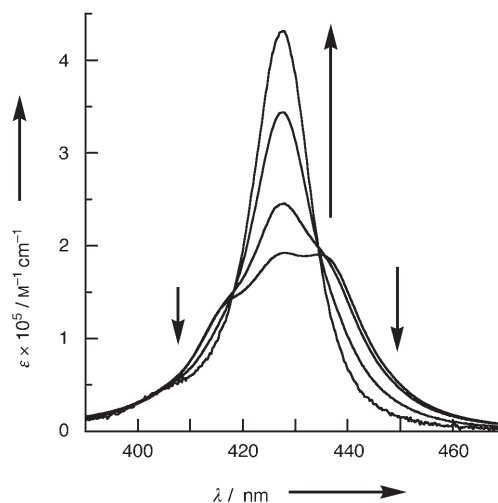
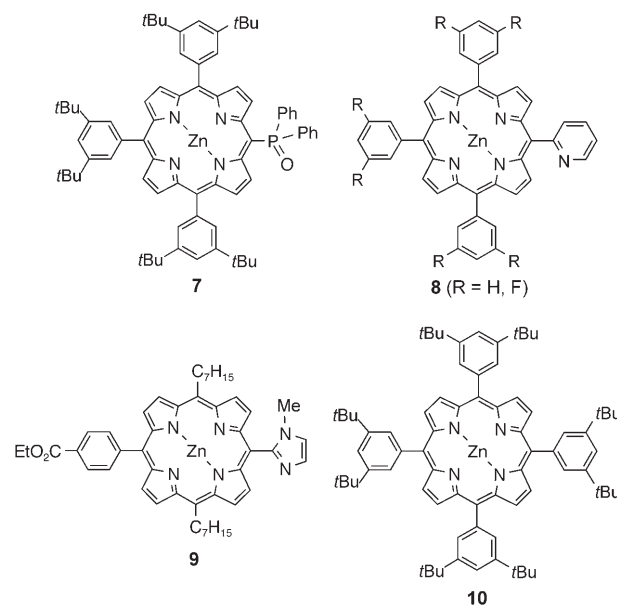


Figure 7. UV/Vis spectra of (*S*)-**4Zn** in toluene at 1.0×10^{-4} – 2.0×10^{-7} M in toluene.

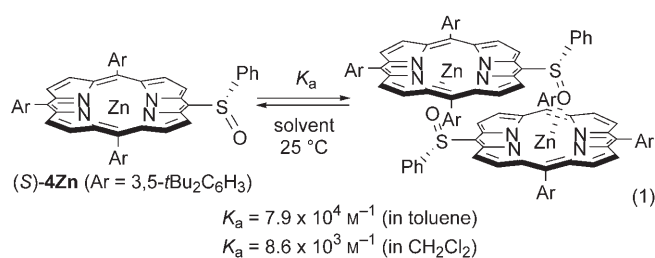
tonic-band-splitting energy^[26,27] (ΔE) of the *S,S* homodimer was determined to be 1100 cm^{-1} .^[28] This value is within the range of those reported for the *P*-oxo-tethered porphyrin **7** dimer ($\Delta E = 940 \text{ cm}^{-1}$),^[9] the 2-pyridyl-tethered porphyrin **8** dimers ($\Delta E = 900$ – 1020 cm^{-1} for $R = \text{H, F}$),^[3d] and the 2-imidazolyl-tethered porphyrin **9** dimer ($\Delta E = 1324 \text{ cm}^{-1}$) (Scheme 5).^[4f]

On the basis of competitive titration experiments with UV/Vis spectroscopy, self-association constants (K_a at 25 °C) for the complementary dimerization of (*S*)-**4Zn** in toluene

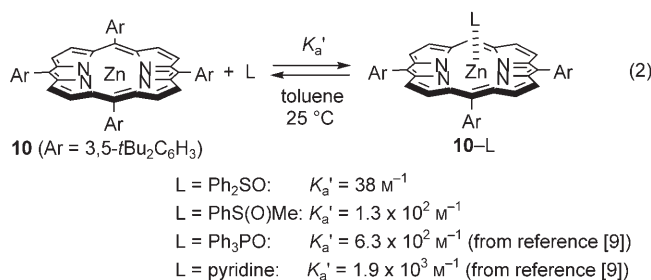


Scheme 5. Structures of porphyrins **7**–**10**.

and dichloromethane were determined as 7.9×10^4 and $8.6 \times 10^3 \text{ M}^{-1}$, respectively (Equation (1)); see also Supporting Information, Figure S12). Owing to the insufficient optical purity (79% *ee*) of (*S*)-**5Zn**, accurate K_a values could not be determined for **5Zn**. However, the concentration dependence of the UV/Vis spectra (see Supporting Information, Figure S13) indicates that the K_a value of (*S*)-**5Zn** in toluene is around 10 times larger than that of (*S*)-**4Zn**. Thus, the *meso*-octylsulfanyl group binds the zinc porphyrins more tightly than the *meso*-phenylsulfanyl group. The solvent effect on the self-association constants can be interpreted in terms of the net dipole moments of the chromophores. In the optimized structures, the dipole moments of the **6** hetero- and homodimers were calculated to be zero and 0.701 D, respectively, which are much smaller than that of the **6** monomer (4.927 D). This suggests that the relative stability of the S-oxo-tethered porphyrin dimer with respect to the monomer increases with decreasing solvent polarity.^[29] Given the ¹H NMR spectroscopic results, the K_a values (at 25 °C) of the **4Zn** heterodimer in toluene and dichloromethane were estimated to be 4.7×10^5 and $5.1 \times 10^4 \text{ M}^{-1}$, respectively.



Notably, the self-association constants of the zinc phenylsulfanylporphyrin **4Zn** are somewhat smaller than that of the zinc diphenylphosphorylporphyrin **7** ($K_a = 5.9 \times 10^6 \text{ M}^{-1}$ in toluene at 25 °C) and significantly smaller than those of the *meso*-2-imidazolylporphyrins reported by Kobuke and co-workers.^[30] To evaluate the coordinating ability of the sulfanyl groups to the zinc center of porphyrins, we also determined association constants (K_a') for the complexation between 5,10,15,20-tetrakis(3,5-di-*tert*-butylphenyl)porphyrinatozinc(II) (**10**) and diorganyl sulfoxides by titration experiments. As shown in Equation (2), the K_a' value of the **10**-OSPh₂ adduct (38 M^{-1} in toluene at 25 °C)^[31] is smaller than that of the **10**-OS(OMe)Ph adduct ($1.3 \times 10^2 \text{ M}^{-1}$). These data indicate that the difference in K_a values between **4Zn** and **5Zn** basically stems from the different coordinating abilities of their sulfanyl ligands. Furthermore, the coordinating abilities of these sulfoxides were found to be weaker than those of triphenylphosphine oxide and pyridine, which exhibited larger K_a' values for the complexation with **10** under the same conditions. Thus, the difference in the self-association constants between **4Zn** and **7** is also ascribed to the different coordinating abilities of the sulfanyl and phosphoryl ligands (see above).



Electrochemical Properties of *meso*-Sulfanylporphyrins

The electrochemical properties of *meso*-sulfanylporphyrins were examined by cyclic voltammetry (CV) and differential pulse voltammetry (DPV) in CH₂Cl₂ with *n*Bu₄NPF₆ (TBAP) as the electrolyte. It is well-known that oxidation of the π ring of a porphyrin monomer occurs through two reversible, one-electron processes. Both *meso*-sulfanylporphyrin **2H₂** and *meso*-sulfanylporphyrin **4H₂** showed reversible voltammograms that are typical of porphyrin monomers. The first and second oxidation potentials of **4H₂** ($E_{1/2} = +0.65$ and $+0.83$ V vs. Fc/Fc⁺; Fc = ferrocene) were observed at lower cathodic potentials than the respective potentials of **2H₂** ($E_{1/2} = +0.54$ and $+0.72$ V vs. Fc/Fc⁺). The difference in the first oxidation potentials ($\Delta E = 0.11$ V) between **4H₂** and **2H₂** is close to that ($\Delta E = 0.115$ V) between 2-phenylsulfanyl-5,10,15,20-tetraphenylporphyrinatocopper(II) and 2-phenylsulfanyl-5,10,15,20-tetraphenylporphyrinatocopper(II) reported by Crossley and co-workers.^[10] These data show that the electron-withdrawing ability of the peripheral sulfanyl substituents is larger than that of the peripheral sulfanyl substituents.

To reveal the effect of dimerization on the electrochemical oxidation processes of zinc sulfanylporphyrins, oxidation potentials of **4Zn** and **5Zn** were also measured by CV and DPV in CH₂Cl₂ at $1.0 \times 10^{-3} \text{ M}$.^[32] At this concentration, **4Zn** and **5Zn** exist mainly as the cofacial dimers. As shown in Figure 8, the **4Zn** dimer was oxidized through three reversible steps with oxidation potentials (E_{ox} vs. Fc/Fc⁺) of $+0.37$, $+0.62$, and $+0.80$ V. The **5Zn** dimer showed similar voltammograms with E_{ox} values of $+0.35$, $+0.61$, and $+0.79$ V (see

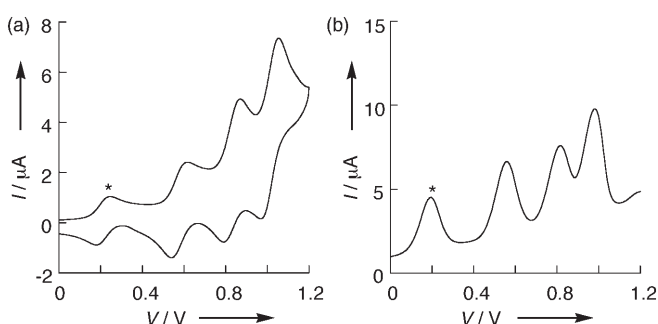


Figure 8. a) Cyclic voltammogram and b) differential pulse voltammogram for **4Zn** recorded in CH₂Cl₂. [**4Zn**] = $1.0 \times 10^{-3} \text{ M}$, [TBAP] = 0.1 M. Scan rate = 20 mV s⁻¹. Asterisks indicate the Fc/Fc⁺ couple.

Supporting Information, Figure S14). In both cases, the first oxidation process of the zinc sulfinylporphyrin dimers is split into two reversible one-electron steps. The differences in oxidation potentials between the first and second steps ($\Delta E_{\text{ox}}=0.25$ V for **4Zn**, 0.26 V for **5Zn**) are close to those observed for the zinc phosphorylporphyrins ($\Delta E_{\text{ox}}=0.22$ –0.25 V). This type of 1e/1e/2e electrochemical oxidation process is well-known for covalently linked cofacial porphyrin dimers. For example, the differences in the first two oxidation steps (ΔE_{ox}) of face-to-face diporphyrins linked by two amide bridges or monolinked by a polyaromatic bridge were reported to be 0.07–0.31 V.^[33] In the case of the present S-oxo-tethered cofacial porphyrin dimers, the initially formed π radical cations seem to delocalize efficiently between the two porphyrin rings through π – π electronic interactions. On the other hand, the second oxidation process occurs by a reversible two-electron step, which implies that the two porphyrin π radical cations interact very weakly or dissociate to the respective monomers. Addition of diorganyl sulfoxides (R_2SO ; R=Ph, Me) to the solution changed the voltammograms of **4Zn** and **5Zn** considerably. In the presence of excess amounts (500 equiv) of the sulfoxides, both the first and second oxidation processes proceeded irreversibly. The first oxidation potentials of the **4Zn**–OSPh₂ and **5Zn**–OSMe₂ adducts were determined by DPV measurements as +0.42 and +0.39 V (vs. Fc/Fc⁺), respectively.

The electrochemical oxidation processes of the S-oxo-tethered zinc porphyrin dimers resemble those of the P-oxo-tethered dimers but differ considerably from those reported for the 2-pyridyl- and 2-imidazolyl-tethered dimers **8** and **9**.^[34] In these N-tethered systems, both the first and second oxidation processes occur through two reversible one-electron steps. Presumably, the sulfinyl linkers of **4Zn** and **5Zn** are not capable of connecting the porphyrin radical cations so as to influence their second oxidation processes, whereas the 2-imidazolyl and 2-pyridyl linkers keep the dimeric structure even in the second oxidation process. This different electrochemical behavior may be attributed to the difference in basicity between the S-oxo ligands and the aromatic N ligands.

Conclusions

We have established a general method for the synthesis of meso-sulfinylporphyrins and succeeded in resolving optically active zinc sulfinylporphyrins for the first time. In weakly polar solvents, the zinc sulfinylporphyrins underwent self-organization to afford cofacial porphyrin dimers through complementary S-oxo–zinc coordination. More importantly, the peripheral S chirality proved to affect the self-aggregation behavior of zinc sulfinylporphyrins. The *S,R* hetero- and *S,S/R,R* homodimers are linked with *C_i* and *C₂* symmetry, respectively, and the helical structure of the homodimers is confirmed by large Cotton effects in their CD spectra. The present study demonstrates that third-row heteroatom–oxo groups are promising ligands for investigating the effects of

peripherally attached chiral auxiliaries on metal-assisted porphyrin self-assemblies.

Experimental Section

General

¹H NMR spectra were recorded on JEOL EX400 and AS300 spectrometers. Chemical shifts are reported relative to TMS. Matrix-assisted laser desorption/ionization (MALDI) time-of-flight (TOF) and ESI mass spectra were recorded on a Shimadzu Kratos Compact MALDI I spectrometer and an Applied Biosystems Mariner biospectrometry workstation, respectively. IR spectra were recorded on a Shimadzu FTIR-8200A spectrophotometer with samples prepared as Nujol mulls. UV/Vis spectra were obtained on a Perkin–Elmer Lambda 900UV/Vis/NIR spectrometer. CD spectra were recorded on a JASCO J-800 spectropolarimeter. Toluene and CH₂Cl₂ were distilled from CaH₂ before use. 5-Iodo-10,15,20-tris(3,5-di-*tert*-butylphenyl)porphyrinatozinc(II) (**1Zn**) was prepared according to the reported procedure.^[16] Other chemicals and solvents were of reagent grade and were purchased commercially and used without further purification. Thin-layer chromatography and flash column chromatography were performed with Art. 5554 DC-Alufolien Kieselgel 60 F₂₅₄ (Merck) and silica gel 60N (Kanto Chemicals), respectively. All reactions were performed under argon atmosphere unless otherwise stated.

Syntheses

2Zn: A 50-mL two-necked round-bottomed flask was charged with **1Zn** (200 mg, 190 μmol), copper(I) iodide (10.9 mg, 57 μmol), neocuproine (12.4 mg, 57 μmol), and sodium *tert*-butoxide (80.0 mg, 830 μmol). The flask was then evacuated on a vacuum line and purged with argon. After toluene (10 mL) and benzenethiol (43 μL , 410 μmol) were added, the mixture was heated under reflux for 5 h. The resulting mixture was cooled to room temperature and filtered through celite. The filtrate was evaporated to leave a solid residue, which was subjected to chromatography on a silica-gel column with hexane/CH₂Cl₂ (4:1) as eluent. [5-Phenylsulfanyl-10,15,20-tris(3,5-di-*tert*-butylphenyl)porphyrinato]zinc(II) (**2Zn**) was obtained as a purple solid (184 mg, 94%) after reprecipitation from CH₂Cl₂/MeOH. UV/Vis (toluene): λ (ϵ) = 429 (350000), 554 (19000), 595 nm (4900 $\text{M}^{-1}\text{cm}^{-1}$); ¹H NMR (CDCl₃, 400 MHz, 298 K): δ = 1.51 (s, 18H; *t*Bu), 1.52 (s, 36H; *t*Bu), 6.96–6.98 (m, 1H; *p*-Ph), 7.03–7.12 (m, 4H; *o,m*-Ph), 7.79–7.80 (m, 3H; *p*-Ar), 8.05 (d, *J* = 2.0 Hz, 2H; *o*-Ar), 8.06 (d, *J* = 2.0 Hz, 4H; *o*-Ar), 8.95 (d, *J* = 4.4 Hz, 2H; 13,17- β), 8.98 (d, *J* = 4.8 Hz, 2H; 12,18- β), 9.02 (d, *J* = 5.2 Hz, 2H; 2,8- β), 9.99 ppm (d, *J* = 4.8 Hz, 2H; 3,7- β); MS (MALDI-TOF): *m/z* = 1046 [*M*]⁺.

2H₂: TFA (30 μL , 380 μmol) was added to a solution of **2Zn** (80 mg, 77 μmol) in CH₂Cl₂ (30 mL), and the resulting mixture was stirred for 3 h at room temperature. The mixture was then washed with aqueous Na₂CO₃ and water, dried over Na₂SO₄, and evaporated to leave a solid residue, which was subjected to chromatography on a silica-gel column with hexane/CH₂Cl₂ (3:1) as eluent. 5-Phenylsulfanyl-10,15,20-tris(3,5-di-*tert*-butylphenyl)porphyrin (**2H₂**) was obtained as a purple solid (74 mg, 98%) after reprecipitation from CH₂Cl₂/MeOH. UV/Vis (toluene): λ (ϵ) = 425 (220000), 520 (12000), 556 (6500), 595 (3900), 651 nm (2600 $\text{M}^{-1}\text{cm}^{-1}$); ¹H NMR (CDCl₃, 400 MHz, 298 K): δ = –2.53 (s, 2H; NH) 1.51 (s, 18H; *t*Bu), 1.52 (s, 36H; *t*Bu), 6.95–6.98 (m, 1H; *p*-Ph), 7.02–7.09 (m, 4H; *o,m*-Ph), 7.78–7.80 (m, 3H; *p*-Ar), 8.04 (d, *J* = 1.2 Hz, 2H; *o*-Ar), 8.05 (d, *J* = 1.6 Hz, 4H; *o*-Ar), 8.83 (d, *J* = 4.4 Hz, 2H; 13,17- β), 8.87 (d, *J* = 4.4 Hz, 2H; 12,18- β), 8.91 (d, *J* = 4.4 Hz, 2H; 2,8- β), 9.86 ppm (d, *J* = 4.8 Hz, 2H; 3,7- β); MS (MALDI-TOF): *m/z* = 984 [*M*]⁺.

3Zn: This compound was prepared from **1Zn** (100 mg, 94 μmol), CuI (5.4 mg, 28 μmol), neocuproine (6.1 mg, 28 μmol), sodium *tert*-butoxide (40.0 mg, 420 μmol), and *n*-octanethiol (36 μL , 210 μmol) according to the procedure described for the synthesis of **2Zn**. [5-*n*-Octylsulfanyl-10,15,20-tris(3,5-di-*tert*-butylphenyl)porphyrinato]zinc(II) (**3Zn**) was obtained as a purple solid (80 mg, 80%). UV/Vis (toluene): λ (ϵ) = 427 (480000), 554 (22000), 595 nm (5400 $\text{M}^{-1}\text{cm}^{-1}$); ¹H NMR (CDCl₃,

400 MHz, 298 K): $\delta=0.78$ (t, $J=6.8$ Hz, 3H; CH_2CH_3), 1.18–1.19 (m, 10H; CH_2), 1.51 (s, 18H; *t*Bu), 1.54 (s, 36H; *t*Bu), 1.73 (tt, $J=6.9$, 6.9 Hz, 2H; SCH_2CH_2), 3.53 (t, $J=7.4$ Hz, 2H; SCH_2), 7.77 (t, $J=2.0$ Hz, 1H; *p*-Ar), 7.81 (t, $J=1.8$ Hz, 2H; *p*-Ar), 8.05 (d, $J=1.6$ Hz, 2H; *o*-Ar), 8.08 (d, $J=2.0$ Hz, 4H; *o*-Ar), 8.95 (d, $J=4.4$ Hz, 2H; 13,17- β), 8.97 (d, $J=4.8$ Hz, 2H; 12,18- β), 9.07 (d, $J=5.2$ Hz, 2H; 2,8- β), 10.12 ppm (d, $J=4.4$ Hz, 2H; 3,7- β); MS (MALDI-TOF): $m/z=1082$ [M] $^+$.

3H₂: This compound was prepared from **3Zn** (30 mg, 28 μmol) and TFA (10.8 μL , 140 μmol) according to the procedure described for the synthesis of **2H₂**. 5-Octylsulfanyl-10,15,20-tris(3,5-di-*tert*-butylphenyl)porphyrin (**3H₂**) was obtained as a purple solid (21 mg, 73%). UV/Vis (toluene): λ (ϵ)=424 (400000), 520 (18000), 555 (10000), 596 (5400), 651 nm ($3800\text{ m}^{-1}\text{ cm}^{-1}$); $^1\text{H NMR}$ (CDCl_3 , 300 MHz, 298 K): $\delta=-2.66$ (s, 2H; NH), 0.78 (t, $J=6.9$ Hz, 3H; CH_2CH_3), 1.16 (br s, 10H; CH_2), 1.51 (s, 18H; *t*Bu), 1.54 (s, 36H; *t*Bu), 1.60–1.74 (m, 2H; SCH_2CH_2), 3.49 (t, $J=7.4$ Hz, 2H; SCH_2), 7.77 (s, 1H; *p*-Ar), 7.81 (s, 2H; *p*-Ar), 8.04 (s, 2H; *o*-Ar), 8.07 (s, 4H; *o*-Ar), 8.85 (s, 4H; 12,13,17,18- β), 8.95 (d, $J=4.8$ Hz, 2H; 2,8- β), 9.98 ppm (d, $J=4.8$ Hz, 2H; 3,7- β); MS (MALDI-TOF): $m/z=1020$ [M] $^+$.

4Zn: A mixture of **2Zn** (41 mg, 39 μmol), *m*CPBA (22 mg, 97 μmol), and CH_2Cl_2 (1 mL) was stirred for 3 h at 0°C. The resulting mixture was washed with aqueous NaOH (1 M) and water and dried over Na_2SO_4 . The solvent was removed by evaporation to leave a solid residue, which was subjected to chromatography on a silica-gel column with hexane/ CH_2Cl_2 (2:1–1:2) as eluent. After reprecipitation from $\text{CH}_2\text{Cl}_2/\text{MeOH}$, [5-phenylsulfanyl-10,15,20-tris(3,5-di-*tert*-butylphenyl)porphyrinato]zinc(II) (**4Zn**) was obtained as a purple solid (26 mg, 62%). UV/Vis (toluene, 5.0×10^{-6} M): λ (ϵ)=428 (240000), 563 (17000), 614 nm ($8800\text{ m}^{-1}\text{ cm}^{-1}$); $^1\text{H NMR}$: monomer ($\text{CDCl}_3/\text{CD}_3\text{OD}=5:1$ v/v, 400 MHz, 298 K): $\delta=1.52$ (s, 18H; *t*Bu), 1.53 (s, 36H; *t*Bu), 7.29–7.31 (m, 3H; *m,p*-Ph), 7.61 (d, $J=7.2$ Hz, 2H; *o*-Ph), 7.79–7.80 (m, 3H; *p*-Ar), 8.03 (d, $J=1.2$ Hz, 4H; *o*-Ar), 8.04 (d, $J=2.0$ Hz, 2H; *o*-Ar), 8.84 (d, $J=4.4$ Hz, 2H; 13,17- β), 8.89 (d, $J=5.2$ Hz, 2H; 12,18- β), 8.96 (d, $J=4.8$ Hz, 2H; 2,8- β), 9.83 ppm (d, $J=5.2$ Hz, 2H; 3,7- β); heterodimer (CD_2Cl_2 , 270 MHz, 263 K): $\delta=1.37$ (s, 9H; *t*Bu), 1.49 (s, 9H; *t*Bu), 1.51 (s, 9H; *t*Bu), 1.60 (s, 9H; *t*Bu), 1.61 (s, 9H; *t*Bu), 1.68 (s, 9H; *t*Bu), 5.60 (d, $J=7.9$ Hz, 2H; *o*-Ph), 6.19 (d, $J=4.3$ Hz, 1H; 3- β), 6.43–6.47 (m, 2H; *m*-Ph), 6.60–6.64 (m, 1H; *p*-Ph), 7.63 (s, 1H; Ar), 7.82 (d, $J=4.3$ Hz, 1H; 2- β), 7.84 (s, 2H; Ar), 7.88 (s, 1H; Ar), 7.99 (s, 1H; Ar), 8.01 (s, 1H; Ar), 8.20 (d, $J=4.3$ Hz, 1H; 7- β), 8.33 (s, 2H; Ar), 8.74 (s, 1H; Ar), 8.74 (d, $J=4.3$ Hz, 1H; 8- β), 8.81 (d, $J=4.6$ Hz, 1H; pyrrole- β), 8.94 (d, $J=4.6$ Hz, 1H; pyrrole- β), 9.00 ppm (s, 2H; pyrrole- β); heterodimer ($[\text{D}_8]\text{toluene}$, 400 MHz, 298 K): $\delta=1.33$ (s, 9H; *t*Bu), 1.45 (s, 9H; *t*Bu), 1.47 (s, 9H; *t*Bu), 1.59 (s, 9H; *t*Bu), 1.64 (s, 9H; *t*Bu), 1.81 (s, 9H; *t*Bu), 5.40 (d, $J=7.6$ Hz, 2H; *o*-Ph), 5.53 (t, $J=7.6$ Hz, 2H; *m*-Ph), 5.85 (t, $J=7.6$ Hz, 1H; *p*-Ph), 6.69 (d, $J=4.4$ Hz, 1H; 3- β), 7.71 (s, 1H; Ar), 7.97 (s, 2H; Ar), 8.00 (s, 1H; Ar), 8.15 (s, 1H; Ar), 8.21 (s, 2H; 2- β), 8.60 (d, $J=4.4$ Hz, 1H; 7- β), 8.71 (s, 1H; Ar), 8.74 (s, 1H; Ar), 9.14 (d, $J=4.0$ Hz, 1H; pyrrole- β), 9.17 (s, 1H; Ar), 9.22 (s, 2H; 8- β , pyrrole- β), 9.26 (d, $J=4.0$ Hz, 1H; pyrrole- β), 9.32 ppm (s, 1H; pyrrole- β); homodimer (CD_2Cl_2 , 270 MHz, 233 K): $\delta=1.36$ (s, 9H; *t*Bu), 1.50 (s, 18H; *t*Bu), 1.59 (s, 9H; *t*Bu), 1.64 (s, 9H; *t*Bu), 1.75 (s, 9H; *t*Bu), 5.58 (d, $J=7.6$ Hz, 2H; *o*-Ph), 6.27 (d, $J=4.9$ Hz, 1H; 3- β), 6.51 (dd, $J=7.6$, 7.4 Hz, 2H; *m*-Ph), 6.70 (d, $J=7.4$ Hz, 1H; *p*-Ph), 7.61 (s, 1H; Ar), 7.77 (s, 1H; Ar), 7.86 (s, 1H; Ar), 7.91 (d, $J=4.6$ Hz, 1H; 7- β), 7.96 (s, 2H; Ar), 8.01 (d, $J=4.9$ Hz, 1H; 2- β), 8.17 (s, 1H; Ar), 8.21 (s, 1H; Ar), 8.45 (s, 1H; Ar), 8.58 (d, $J=4.6$ Hz, 1H; 8- β), 8.66 (s, 1H; Ar), 8.93 (s, 1H; pyrrole- β), 8.96 (s, 1H; pyrrole- β), 9.03 (d, $J=4.9$ Hz, 1H; pyrrole- β), 9.09 ppm (d, $J=4.9$ Hz, 1H; pyrrole- β); pyridine adduct ($\text{CDCl}_3/[\text{D}_5]\text{pyridine}$, 400 MHz, 298 K): $\delta=1.50$ (s, 36H; *t*Bu), 1.51 (s, 18H; *t*Bu), 7.18–7.20 (m, 3H; *m,p*-Ph), 7.51–7.54 (m, 2H; *o*-Ph), 7.75–7.76 (m, 3H; *p*-Ar), 7.98–8.00 (m, 6H; *o*-Ar), 8.83 (d, $J=4.4$ Hz, 2H; 13,17- β), 8.87 (d, $J=4.4$ Hz, 2H; 12,18- β), 8.94 (d, $J=4.8$ Hz, 2H; 2,8- β), 9.94 ppm (d, $J=4.8$ Hz, 2H; 3,7- β); MS (MALDI-TOF): $m/z=1063$ [M] $^+$, 1047 [$M-\text{O}$] $^+$; MS (ESI): $m/z=2148$ [$2M+\text{Na}$] $^+$.

4H₂: This compound was prepared from 1) **4Zn** (20 mg, 19 μmol) and TFA (7.3 μL , 95 μmol) and 2) **2H₂** (10 mg, 10 μmol) and *m*CPBA (3.5 mg, 15 μmol) according to the procedures described for the synthesis of **2H₂** and **4Zn**, respectively. 5-Phenylsulfanyl-10,15,20-tris(3,5-di-*tert*-butylphen-

yl)porphyrin (**4H₂**) was obtained as a purple solid (8.1 mg, 43% from **4Zn**; 7.9 mg, 79% from **2H₂**). UV/Vis (toluene): λ (ϵ)=424 (410000), 520 (18000), 555 (9800), 591 (6700), 646 nm ($4700\text{ m}^{-1}\text{ cm}^{-1}$); $^1\text{H NMR}$ (CDCl_3 , 300 MHz, 298 K): $\delta=-2.57$ (s, 2H; NH), 1.51 (s, 18H; *t*Bu), 1.52 (s, 36H; *t*Bu), 7.22–7.26 (m, 3H; *m,p*-Ph), 7.64 (dd, $J=8.1$, 1.5 Hz, 2H; *o*-Ph), 7.80–7.81 (m, 3H; *p*-Ar), 8.02–8.03 (m, 6H; *o*-Ar), 8.83 (d, $J=4.8$ Hz, 2H; 13,17- β), 8.86 (d, $J=4.8$ Hz, 2H; 12,18- β), 8.96 (d, $J=4.8$ Hz, 2H; 2,8- β), 9.98 ppm (d, $J=4.8$ Hz, 2H; 3,7- β); MS (MALDI-TOF): $m/z=1000$ [M] $^+$, 984 [$M-\text{O}$] $^+$, 923 [$M-\text{Ph}$] $^+$, 875 [$M-\text{S}(\text{O})\text{Ph}$] $^+$.

5Zn: This compound was prepared from **3Zn** (10 mg, 9.3 μmol) and *m*CPBA (3.1 mg, 14 μmol) according to the procedure described for the synthesis of **4Zn**. [5-*n*-Octylsulfanyl-10,15,20-tris(3,5-di-*tert*-butylphenyl)porphyrinato]zinc(II) (**5Zn**) was isolated as a purple solid (8.2 mg, 80%). UV/Vis (toluene, 2.0×10^{-7} M): λ (ϵ)=427 (180000), 563 (13000), 614 nm ($7600\text{ m}^{-1}\text{ cm}^{-1}$); $^1\text{H NMR}$: monomer ($\text{CDCl}_3/\text{CD}_3\text{OD}=5:2$ v/v, 400 MHz, 298 K): $\delta=0.73$ (t, $J=6.8$ Hz, 3H; CH_2CH_3), 1.06–1.07 (m, 10H; CH_2), 1.53 (s, 18H; *t*Bu), 1.55 (s, 36H; *t*Bu), 1.70–1.71 (m, 2H; SCH_2CH_2), 3.65 (br s, 1H; SCH_2), 4.04 (br s, 1H; SCH_2), 7.80 (t, $J=1.8$ Hz, 1H; *p*-Ar), 7.83 (t, $J=1.8$ Hz, 2H; *p*-Ar), 8.08 (s, 6H; *o*-Ar), 8.87 (d, $J=4.8$ Hz, 2H; 13,17- β), 8.92 (d, $J=4.8$ Hz, 2H; 12,18- β), 9.00 (s, 2H; 2,8- β), 9.88 ppm (br s, 2H; 3,7- β); heterodimer (CD_2Cl_2 , 400 MHz, 298 K): $\delta=1.94$ –1.98 (m, 1H; SCH_2), 2.18–2.22 (m, 1H; SCH_2), 6.50 (d, $J=4.4$ Hz, 1H; 3- β), 7.74 (d, $J=1.5$ Hz, 1H; Ar), 7.87 (t, $J=1.7$ Hz, 1H; Ar), 7.90–7.91 (m, 2H; Ar), 7.98 (d, $J=4.9$ Hz, 1H; 7- β), 7.98 (d, $J=4.4$ Hz, 1H; 2- β), 8.01 (t, $J=1.5$ Hz, 1H; Ar), 8.03 (t, $J=1.7$ Hz, 1H; Ar), 8.31–8.32 (m, 2H; Ar), 8.66 (d, $J=4.9$ Hz, 1H; 8- β), 8.79 (d, $J=1.5$ Hz, 1H; Ar), 8.85 (d, $J=4.4$ Hz, 1H; pyrrole- β), 8.93 (d, $J=4.9$ Hz, 1H; pyrrole- β), 8.94 (d, $J=4.9$ Hz, 1H; pyrrole- β), 8.96 ppm (d, $J=4.4$ Hz, 1H; pyrrole- β); homodimer (CD_2Cl_2 , 400 MHz, 298 K): $\delta=1.94$ –1.98 (m, 1H; SCH_2), 2.30–2.34 (m, 1H; SCH_2), 6.61 (d, $J=4.4$ Hz, 1H; 3- β), 7.73 (d, $J=4.4$ Hz, 1H; 7- β), 8.14 (d, $J=4.4$ Hz, 1H; 2- β), 8.71 ppm (d, $J=4.4$ Hz, 1H; 8- β); due to the low S/N ratio, other peaks could not be assigned clearly; pyridine adduct ($\text{CDCl}_3/[\text{D}_5]\text{pyridine}$, 400 MHz, 243 K): $\delta=0.78$ (t, $J=6.8$ Hz, 3H; CH_2CH_3), 1.12 (s, 10H; CH_2), 1.49 (s, 9H; *t*Bu), 1.51 (s, 18H; *t*Bu), 1.53 (s, 18H; *t*Bu), 1.55 (s, 9H; *t*Bu), 1.63–1.69 (m, 1H; SCH_2CH_2), 1.83–1.89 (m, 1H; SCH_2CH_2), 3.54–3.60 (m, 1H; SCH_2), 4.14–4.19 (m, 1H; SCH_2), 7.74 (s, 1H; *p*-Ar), 7.77 (s, 2H; *p*-Ar), 7.95 (s, 1H; *o*-Ar), 7.98 (s, 1H; *o*-Ar), 8.02 (s, 1H; *o*-Ar), 8.06 (s, 2H; *o*-Ar), 8.13 (s, 1H; *o*-Ar), 8.91–8.94 (m, 4H; 12,13,17,18- β), 9.08 (s, 2H; 2,8- β), 9.83 (d, $J=4.0$ Hz, 1H; 3- β), 10.55 ppm (d, $J=4.0$ Hz, 1H; 7- β); MS (MALDI-TOF): $m/z=1099$ [M] $^+$, 1083 [$M-\text{O}$] $^+$, 987 [$M-\text{C}_8\text{H}_{17}$] $^+$; MS (ESI): $m/z=2220$ [$2M+\text{Na}$] $^+$.

5H₂: This compound was prepared from **3H₂** (20 mg, 20 μmol) and *m*CPBA (5.2 mg, 24 μmol) according to the procedure described for the synthesis of **4H₂** from **2H₂**. 5-Octylsulfanyl-10,15,20-tris(3,5-di-*tert*-butylphenyl)porphyrin (**5H₂**) was obtained as a purple solid (14 mg, 68%). UV/Vis (toluene): λ (ϵ)=424 (400000), 519 (17800), 555 (9500), 592 (6000), 647 nm ($3900\text{ m}^{-1}\text{ cm}^{-1}$); $^1\text{H NMR}$ (CDCl_3 , 300 MHz, 298 K): $\delta=-2.65$ (s, 2H; NH), 0.77 (t, $J=6.8$ Hz, 3H; CH_2CH_3), 1.15 (br s, 10H; CH_2), 1.51 (s, 18H; *t*Bu), 1.54 (s, 36H; *t*Bu), 1.63–1.69 (m, 1H; SCH_2CH_2), 1.87–1.93 (m, 1H; SCH_2CH_2), 3.52–3.58 (m, 1H; SCH_2), 4.03–4.09 (m, 1H; SCH_2), 7.79 (s, 1H; *p*-Ar), 7.82 (s, 2H; *p*-Ar), 8.03–8.08 (m, 6H; *o*-Ar), 8.84–8.88 (m, 4H; 12,13,17,18- β), 9.01 (d, $J=4.4$ Hz, 2H; 2,8- β), 10.18 ppm (br s, 2H; 3,7- β); MS (MALDI-TOF): $m/z=1036$ [M] $^+$, 1020 [$M-\text{O}$] $^+$, 923 [$M-\text{C}_8\text{H}_{17}$] $^+$.

Optical Resolution of Zinc Sulfanylporphyrins

Optical resolution of the racemates of **4Zn** and **5Zn** was performed on a Shimadzu Proinence GPC system equipped with a preparative chiral HPLC column (DAICEL Chiralpak IA; 250 \times 10 mm) with hexane/2-propanol (100:1) as eluent. The flow rate and temperature were kept at 1.0 mL min $^{-1}$ and 25°C, respectively. The enantiomeric excess was determined by comparison of the peak areas of two fractions. Although the reason is unclear at present, **5Zn** could not be resolved completely.

Determination of K_a of Zinc Sulfanylporphyrins

The K_a values of the optically active **4Zn** homodimer (listed in [Eq. (1)]) were determined by the competitive-titration method with UV/Vis spectroscopy at 25°C. The observed spectral changes in the titration experi-

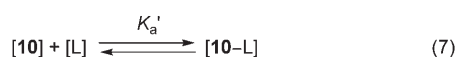
ments (for a representative result, see Supporting Information, Figure S12) were analyzed by using SPECFIT^[35] according to Equations (3)–(6), in which [M], [D], [M–L], and [L] refer to the concentrations of the



$$K_a = \frac{[D]}{[M]^2} \quad (5)$$

$$K_a'' = \frac{[M-L]}{[M][L]} \quad (6)$$

(*S*)-**4Zn** monomer, the (*S*)-**4Zn** homodimer, the (*S*)-**4Zn**-OSPh₂ adduct, and diphenyl sulfoxide, respectively. In these analyses, the association constants between the **4Zn** monomer and diphenyl sulfoxide (K_a'') in toluene and dichloromethane were also determined as 49 and 17 M⁻¹, respectively. The association constants between **10** and diorganyl sulfoxides (K_a') listed in Equation (2) were also determined by the titration measurements according to Equations (7) and (8), in which [L] refers to the



$$K_a' = \frac{[10-L]}{[10][L]} \quad (8)$$

concentration of diorganyl sulfoxides (OS(R)Ph; R = Ph, *n*-C₈H₁₇). The self-association constants of the **4Zn** heterodimers were calculated on the basis of the hetero-/homodimer ratios of the **4Zn** racemate and the K_a values of the **4Zn** homodimer. The approximate K_a values of the **5Zn** homodimer were determined by spectral-shape analysis at several concentrations by using ORIGIN. It was found that the K_a value of the **5Zn** homodimer is around 10 times larger than that of the **4Zn** homodimer.

Determination of Oxidation Potentials of Zinc Sulfinylporphyrins

Electrochemical measurements were performed on a CH Instruments model 660A electrochemical workstation with a glassy carbon working electrode, a platinum wire counterelectrode, and an Ag/Ag⁺ (0.01 M AgNO₃, 0.1 M *n*Bu₄NPF₆ in MeCN) reference electrode. The potentials were calibrated with Fc/Fc⁺ ($E_{\text{mid}} = +0.20$ V vs. Ag/Ag⁺). The number of electrons for the oxidation processes was approximated by comparison of the peak areas for both CV and DPV, although an unavoidable error is involved due to an overlap between the second and third peaks. As no further oxidation step was observed with a wider sweep, we concluded that the electrochemical oxidation of zinc sulfinylporphyrins occurs through 1e/1e/2e processes as was observed for zinc phosphorylporphyrins.^[9]

DFT Calculations on Model Compounds

The structures of 5-phenylsulfinyl-10,15,20-triphenylporphyrinatozinc(II) **6** were optimized by using DFT calculations. The basis set used was 6-31G(d,p).^[36] The DFT functionals were the Becke 1988 exchange and the Lee–Yang–Parr correlation functionals (B3LYP).^[37] The optimized structures are depicted in Figure 5, and the bond lengths of the optimized structures are shown in Table 2. All calculations were carried out with the Gaussian 03 suite of programs.^[38]

Acknowledgements

This work was partially supported by Grants-in-Aid (Nos. 17350018 and 19027030) from the Ministry of Education, Culture, Sports, Science, and

Technology of Japan. We thank the following, all of Kyoto University: Prof. Atsuhiko Osuka for use of the ESI mass spectrometer, Prof. Toshio Masuda for use of the CD spectropolarimeter, Mr. Satoru Hiroto and Mr. Yuji Suzuki for assistance with the CD and ESI mass spectral measurements, and Prof. Fumio Sanda and Dr. Yutaka Hitomi for helpful suggestions about the exciton-coupled CD method and the titration measurements, respectively.

- [1] a) J. Deisenhofer, O. Epp, K. Miki, R. Huber, H. Michel, *J. Mol. Biol.* **1984**, *180*, 385; b) *The Photosynthetic Reaction Center* (Eds.: J. Deisenhofer, J. R. Norris), Academic Press, San Diego, **1993**.
- [2] a) J. K. M. Sanders in *Comprehensive Supramolecular Chemistry*, Vol. 9 (Eds.: J. Atwood, E. Davies, D. MacNicol, F. Vögtle, J.-M. Lehn), Pergamon Press, Oxford, **1996**, pp. 131–164; b) V. Balzani, F. Scandola in *Comprehensive Supramolecular Chemistry*, Vol. 10 (Eds.: J. Atwood, E. Davies, D. MacNicol, F. Vögtle, J.-M. Lehn), Pergamon Press, Oxford, **1996**, pp. 687–746; c) J. K. M. Sanders in *The Porphyrin Handbook*, Vol. 3 (Eds.: K. M. Kadish, K. M. Smith, R. Guilard), Academic Press, San Diego, **2000**, pp. 347–368; d) J.-C. Chambron, V. Heitz, J.-P. Sauvage in *The Porphyrin Handbook*, Vol. 6 (Eds.: K. M. Kadish, K. M. Smith, R. Guilard), Academic Press, San Diego, **2000**, pp. 1–42; e) T. Imamura, K. Fukushima, *Coord. Chem. Rev.* **2000**, *198*, 133; f) J. Wojaczyński, L. Latos-Grazyński, *Coord. Chem. Rev.* **2000**, *204*, 113; g) L. Baldini, C. A. Hunter, *Adv. Inorg. Chem.* **2002**, *53*, 213; h) E. Iengo, E. Zangrando, E. Alessio, *Eur. J. Inorg. Chem.* **2003**, 2371; i) P. D. Harvey in *The Porphyrin Handbook*, Vol. 18 (Eds.: K. M. Kadish, K. M. Smith, R. Guilard), Academic Press, San Diego, **2003**, pp. 63–250; j) Y. Kobuke, *J. Porphyrins Phthalocyanines* **2004**, *8*, 156; k) C. M. Drain, I. Goldberg, I. Sylvain, A. Falber, *Top. Curr. Chem.* **2005**, *245*, 55; l) A. Satake, Y. Kobuke, *Tetrahedron* **2005**, *61*, 13; m) T. S. Balaban, *Acc. Chem. Res.* **2005**, *38*, 612; n) H. Imahori, *J. Phys. Chem. B* **2004**, *108*, 6130; o) H. Imahori, *Bull. Chem. Soc. Jpn.* **2007**, *80*, 621, and references therein.
- [3] For examples, see: a) E. B. Fleischer, A. M. Shachter, *Inorg. Chem.* **1991**, *30*, 3763; b) C. A. Hunter, L. D. Sarson, *Angew. Chem.* **1994**, *106*, 2424; *Angew. Chem. Int. Ed. Engl.* **1994**, *33*, 2313; c) C. M. Drain, J.-M. Lehn, *J. Chem. Soc. Chem. Commun.* **1994**, 2313; d) R. T. Stibrany, J. Vasudevan, S. Knapp, J. A. Potenza, T. Emge, H. J. Schugar, *J. Am. Chem. Soc.* **1996**, *118*, 3980; e) L. D. Sarson, K. Ueda, M. Takeuchi, S. Shinkai, *Chem. Commun.* **1996**, 619; f) J. Vasudevan, R. T. Stibrany, J. Bumby, S. Knapp, J. A. Potenza, T. J. Emge, H. J. Schugar, *J. Am. Chem. Soc.* **1996**, *118*, 11676; g) R. V. Slone, J. T. Hupp, *Inorg. Chem.* **1997**, *36*, 5422; h) K. Funatsu, T. Imamura, A. Ichimura, Y. Sasaki, *Inorg. Chem.* **1998**, *37*, 4986; i) J. Fan, J. A. Whiteford, B. Olenyuk, M. D. Levin, P. J. Stang, E. B. Fleischer, *J. Am. Chem. Soc.* **1999**, *121*, 2741; j) A. Prodi, M. T. Indelli, C. J. Kleverlaan, F. Scandola, E. Alessio, T. Gianferrara, L. G. Marzilli, *Chem. Eur. J.* **1999**, *5*, 2668; k) S. L. Darling, C. C. Mak, N. Bampos, N. Feeder, S. J. Teat, J. K. M. Sanders, *New J. Chem.* **1999**, *23*, 359; l) D. Sun, F. S. Tham, C. A. Reed, L. Chaker, M. Burgess, P. D. W. Boyd, *J. Am. Chem. Soc.* **2000**, *122*, 10704; m) A. Tsuda, T. Nakamura, S. Sakamoto, K. Yamaguchi, A. Osuka, *Angew. Chem.* **2002**, *114*, 2941; *Angew. Chem. Int. Ed.* **2002**, *41*, 2817; n) E. Iengo, E. Zangrando, S. Geremia, R. Graff, B. Kieffer, E. Alessio, *Chem. Eur. J.* **2002**, *8*, 4670; o) A. Tsuda, S. Sakamoto, K. Yamaguchi, T. Aida, *J. Am. Chem. Soc.* **2003**, *125*, 15722; p) M. Vinodu, Z. Stein, I. Goldberg, *Inorg. Chem.* **2004**, *43*, 7582.
- [4] For examples, see: a) Y. Kobuke, H. Miyaji, *J. Am. Chem. Soc.* **1994**, *116*, 4111; b) Y. Kobuke, H. Miyaji, *Bull. Chem. Soc. Jpn.* **1996**, *69*, 3563; c) K. Ogawa, Y. Kobuke, *Angew. Chem.* **2000**, *112*, 4236; *Angew. Chem. Int. Ed.* **2000**, *39*, 4070; d) Y. Kobuke, K. Ogawa, *Bull. Chem. Soc. Jpn.* **2003**, *76*, 689; e) R. Takahashi, Y. Kobuke, *J. Am. Chem. Soc.* **2003**, *125*, 2372; f) H. Ozeki, A. Nomoto, K. Ogawa, Y. Kobuke, M. Murakami, K. Hosoda, M. Ohtani, S. Nakashima, H. Miyasaka, T. Okada, *Chem. Eur. J.* **2004**, *10*, 6393; g) F. Hajjaj, Z. S. Yoon, M.-C. Yoon, J. Park, A. Satake, D. Kim, Y. Kobuke, *J. Am. Chem. Soc.* **2006**, *128*, 4612.

- [5] For examples, see: a) J. Mårtensson, K. Sandros, O. Wennerström, *Tetrahedron Lett.* **1993**, *34*, 541; b) S. Knapp, J. Vasudevan, T. J. Emge, B. H. Arison, J. A. Potenza, H. J. Schugar, *Angew. Chem.* **1998**, *110*, 2537; *Angew. Chem. Int. Ed.* **1998**, *37*, 2368; c) M. Gardner, A. J. Guerin, C. A. Hunter, U. Michelsen, C. Rotger, *New J. Chem.* **1999**, *23*, 309.
- [6] For examples, see: a) T. S. Balaban, A. D. Bhise, M. Fischer, M. Linke-Schaetzel, C. Roussel, N. Vanthuyne, *Angew. Chem.* **2003**, *115*, 2190; *Angew. Chem. Int. Ed.* **2003**, *42*, 2140; b) H. Tamiaki, S. Kimura, T. Kimura, *Tetrahedron* **2003**, *59*, 7423; c) T. S. Balaban, M. Linke-Schaetzel, A. D. Bhise, N. Vanthuyne, C. Roussel, *Eur. J. Org. Chem.* **2004**, 3919; d) T. S. Balaban, M. Linke-Schaetzel, A. D. Bhise, N. Vanthuyne, C. Roussel, C. E. Anson, G. Buth, A. Eichhöfer, K. Foster, G. Garab, H. Gliemann, R. Goddard, T. Javorfi, A. K. Powell, H. Rösner, T. Schimmel, *Chem. Eur. J.* **2005**, *11*, 2267.
- [7] For examples, see: a) H. Tamiaki, A. R. Holzwarth, K. Schaffner, *J. Photochem. Photobiol. B* **1992**, *15*, 355; b) M. J. Crossley, L. G. Mackay, A. C. Try, *J. Chem. Soc. Chem. Commun.* **1995**, 1925; c) T. Ema, S. Misawa, S. Nemugaki, T. Sakai, M. Utaka, *Chem. Lett.* **1997**, 487; d) H.-Y. Liu, X.-M. Hu, X. Ying, Y. Liu, J. Huang, J.-W. Huang, X. Tian, L.-N. Ji, *Mater. Sci. Eng. C* **1999**, *10*, 33; e) X. Huang, K. Nakanishi, N. Berova, *Chirality* **2000**, *12*, 237; f) V. V. Borovkov, N. Yamamoto, J. M. Lintuluoto, T. Tanaka, Y. Inoue, *Chirality* **2001**, *13*, 329; g) R. Paolesse, D. Monti, L. La Monica, M. Venanzi, A. Froio, S. Nardis, C. Di Natale, E. Martinelli, A. D'Amico, *Chem. Eur. J.* **2002**, *8*, 2476; h) T. Hayashi, T. Aya, M. Nonoguchi, T. Mizutani, Y. Hisaeda, S. Kitagawa, H. Ogoshi, *Tetrahedron* **2002**, *58*, 2803; i) H. Tamiaki, M. Amakawa, A. R. Holzwarth, K. Schaffner, *Photosynth. Res.* **2002**, *71*, 59; j) V. Huber, M. Katterle, M. Lysetska, F. Würthner, *Angew. Chem.* **2005**, *117*, 3208; *Angew. Chem. Int. Ed.* **2005**, *44*, 3147; k) M. Kunieda, H. Tamiaki, *Eur. J. Org. Chem.* **2006**, 2352; l) C. Röger, M. G. Müller, M. Lysetska, Y. Miloslavina, A. R. Holzwarth, F. Würthner, *J. Am. Chem. Soc.* **2006**, *128*, 6542.
- [8] a) F. Atefi, O. B. Locos, M. O. Senge, D. P. Arnold, *J. Porphyrins Phthalocyanines* **2006**, *10*, 176; b) F. Atefi, J. C. McMurtrie, P. Turner, M. Duriska, D. P. Arnold, *Inorg. Chem.* **2006**, *45*, 6479; c) F. Atefi, J. C. McMurtrie, D. P. Arnold, *Dalton Trans.* **2007**, 2163.
- [9] Y. Matano, K. Matsumoto, Y. Terasaka, H. Hotta, Y. Araki, O. Ito, M. Shiro, T. Sasamori, N. Tokitoh, H. Imahori, *Chem. Eur. J.* **2007**, *13*, 891.
- [10] R. A. Binstead, M. J. Crossley, N. S. Hush, *Inorg. Chem.* **1991**, *30*, 1259.
- [11] a) Y. Deng, C. K. Chang, D. G. Nocera, *Angew. Chem.* **2000**, *112*, 1108; *Angew. Chem. Int. Ed.* **2000**, *39*, 1066; b) L. L. Chng, C. J. Chang, D. G. Nocera, *J. Org. Chem.* **2003**, *68*, 4075; c) L. Yu, K. Muthukumar, I. V. Sazanovich, C. Kirmaier, E. Hindin, J. R. Diers, P. D. Boyle, D. F. Bocian, D. Holtzen, J. S. Lindsey, *Inorg. Chem.* **2003**, *42*, 6629; d) B. Felber, F. Diederich, *Helv. Chim. Acta* **2005**, *88*, 120.
- [12] a) G.-Y. Gao, A. J. Colvin, Y. Chen, X. P. Zhang, *Org. Lett.* **2003**, *5*, 3261; b) Y. Chen, G.-Y. Gao, X. P. Zhang, *Tetrahedron Lett.* **2005**, *46*, 4965.
- [13] a) M. M. Khan, H. Ali, J. E. van Lier, *Tetrahedron Lett.* **2001**, *42*, 1615; b) N. P. Redmore, I. V. Rubtsov, M. J. Therien, *Inorg. Chem.* **2002**, *41*, 566; c) T. Takanami, M. Hayashi, F. Hino, K. Suda, *Tetrahedron Lett.* **2003**, *44*, 7353; d) Y. Chen, X. P. Zhang, *J. Org. Chem.* **2003**, *68*, 4432; e) G.-Y. Gao, Y. Chen, X. P. Zhang, *Org. Lett.* **2004**, *6*, 1837.
- [14] G.-Y. Gao, A. J. Colvin, Y. Chen, X. P. Zhang, *J. Org. Chem.* **2004**, *69*, 8886.
- [15] C. Liu, D.-M. Shen, Q.-Y. Chen, *J. Org. Chem.* **2007**, *72*, 2732.
- [16] F. Odobel, F. Suzenet, E. Blart, J.-P. Quintard, *Org. Lett.* **2000**, *2*, 131.
- [17] C. G. Bates, R. K. Gujadhur, D. Venkataraman, *Org. Lett.* **2002**, *4*, 2803.
- [18] M. J. Crossley, L. G. King, S. M. Pyke, C. W. Tansey, *J. Porphyrins Phthalocyanines* **2002**, *6*, 685.
- [19] In CD₂Cl₂, the signals of the 3,7-β protons of **4H₂** and **5H₂** coalesced at -15 and 25 °C, respectively.
- [20] The nonequivalence of all the β protons is not due to the S chirality itself, because such discrimination was not observed for **4H₂** and **5H₂**.
- [21] M. Calligaris, *Coord. Chem. Rev.* **2004**, *248*, 351.
- [22] If the aggregates consist of *n* pieces (*n* ≥ 3) of sulfinylporphyrins, more than one pair of S-oxo-linked diastereomers can be formed. The spectra shown in Figures 1 b and 2 b imply that the contribution of cyclic, linear, or branched higher oligomers is negligible in solution.
- [23] It is well-known that the *meso*-phenyl rings of tetraphenylporphyrin are not on the same plane of the porphyrin ring due to steric repulsion with neighboring β protons.
- [24] In the primary electron donor P700 of cyanobacterial photosystem I, two chlorin planes of a chlorophyll pair are parallel at an interplanar distance of 3.6 Å and partially overlapping with a center-to-center distance of 6.3 Å; see: P. Jordan, P. Fromme, H. T. Witt, O. Klukas, W. Saenger, N. Krauß, *Nature* **2001**, *411*, 909.
- [25] For examples, see: a) S. Matile, N. Berova, K. Nakanishi, S. Novkova, I. Philipova, B. Blagoev, *J. Am. Chem. Soc.* **1995**, *117*, 7021; b) S. Matile, N. Berova, K. Nakanishi, J. Fleischhauer, R. W. Woody, *J. Am. Chem. Soc.* **1996**, *118*, 5198; c) K. Nakanishi, N. Berova in *Circular Dichroism: Principles and Applications* (Eds.: K. Nakanishi, N. Berova, R. W. Woody), VCH, New York, **1994**, p. 361; d) B. H. Rickman, S. Matile, K. Nakanishi, N. Berova, *Tetrahedron* **1998**, *54*, 5041; e) F. Takei, H. Hayashi, K. Onitsuka, N. Kobayashi, S. Takahashi, *Angew. Chem.* **2001**, *113*, 4216; *Angew. Chem. Int. Ed.* **2001**, *40*, 4092; f) J. Tabei, M. Shiotsuki, F. Sanda, T. Masuda, *Macromolecules* **2005**, *38*, 9448.
- [26] M. Kasha, H. R. Rawls, M. A. El-Bayoumi, *Pure Appl. Chem.* **1965**, *11*, 371.
- [27] For discussions on the excitonic coupling of covalently and noncovalently linked porphyrin dimers, see: a) R. R. Bucks, S. G. Boxer, *J. Am. Chem. Soc.* **1982**, *104*, 340; b) A. Osuka, K. Maruyama, *J. Am. Chem. Soc.* **1988**, *110*, 4454; c) B. C. Bookser, T. C. Bruce, *J. Am. Chem. Soc.* **1991**, *113*, 4208.
- [28] The absorption spectra, in which energies are given in cm⁻¹, were deconvoluted into three Gaussian bands and analyzed by ORIGIN.
- [29] The *E_T* values of dichloromethane and toluene are 40.7 and 33.9, respectively; see: C. Reichardt, *Chem. Rev.* **1994**, *94*, 2319.
- [30] For instance, the *K_a* value of **9** was reported to be about 10¹¹ M⁻¹ in CHCl₃ at 25 °C; see reference [4].
- [31] This value is close to the association constant of (*S*)-**4Zn**-OSPh₂ adduct (49 M⁻¹ in toluene at 25 °C) determined by competitive titration; see Experimental Section.
- [32] In the electrochemical measurements, the racemates of **4Zn** and **5Zn** were used. Thus, the voltammograms depicted in Figure 8 and Figure S14 of the Supporting Information are superimpositions of those of the homo- and heterodimers, although the differences in their oxidation potentials are considered to be very small.
- [33] Y. Le Mest, M. L'Her, N. H. Hendricks, K. Kim, J. P. Collman, *Inorg. Chem.* **1992**, *31*, 835; the authors systematically investigated the electrochemical and spectroscopic properties of two families of dimeric porphyrins and revealed the important role of electronic π-π interactions in their mixed-valence behavior.
- [34] The Schugar dimer **8** showed four separate one-electron oxidation potentials at +0.56, +1.01, +1.21, and +1.55 V (vs. saturated calomel electrode (SCE); in CH₂Cl₂ containing *n*Bu₄NBF₄)^[31] and the Kobuke dimer **9** revealed oxidation potentials at +0.414, +0.632, +0.968, and +1.120 V (vs. Ag/Ag⁺; in CHCl₃ containing TBAP)^[40] The oxidation potentials of **4Zn** and **5Zn** versus SCE were calculated to be +0.77, +1.02, +1.20 V and +0.75, +1.01, +1.19 V, respectively.
- [35] R. A. Binstead, A. D. Zuberbühler, SPECFIT Global Analysis System 2.10 (Rev. X), Spectrum Software Associates, Chapel Hill, NC (USA), **1998**.

- [36] a) R. Krishnan, J. S. Binkley, R. Seeger, J. A. Pople, *J. Chem. Phys.* **1980**, *72*, 650; b) A. D. McLean, G. S. Chandler, *J. Chem. Phys.* **1980**, *72*, 5639.
- [37] a) A. D. Becke, *J. Chem. Phys.* **1993**, *98*, 5648; b) C. Lee, W. Yang, R. G. Parr, *Phys. Rev. B* **1988**, *37*, 785.
- [38] M. J. Frisch, G. W. Trucks, H. B. Schlegel, G. E. Scuseria, M. A. Robb, J. R. Cheeseman, J. A. Montgomery, Jr., T. Vreven, K. N. Kudin, J. C. Burant, J. M. Millam, S. S. Iyengar, J. Tomasi, V. Barone, B. Mennucci, M. Cossi, G. Scalmani, N. Rega, G. A. Petersson, H. Nakatsuji, M. Hada, M. Ehara, K. Toyota, R. Fukuda, J. Hasegawa, M. Ishida, T. Nakajima, Y. Honda, O. Kitao, H. Nakai, M. Klene, X. Li, J. E. Knox, H. P. Hratchian, J. B. Cross, C. Adamo, J. Jaramillo, R. Gomperts, R. E. Stratmann, O. Yazyev, A. J. Austin, R. Cammi, C. Pomelli, J. W. Ochterski, P. Y. Ayala, K. Morokuma, G. A. Voth, P. Salvador, J. J. Dannenberg, V. G. Zakrzewski, S. Dapprich, A. D. Daniels, M. C. Strain, O. Farkas, D. K. Malick, A. D. Rabuck, K. Raghavachari, J. B. Foresman, J. V. Ortiz, Q. Cui, A. G. Baboul, S. Clifford, J. Cioslowski, B. B. Stefanov, G. Liu, A. Liashenko, P. Piskorz, I. Komaromi, R. L. Martin, D. J. Fox, T. Keith, M. A. Al-Laham, C. Y. Peng, A. Nanayakkara, M. Challacombe, P. M. W. Gill, B. Johnson, W. Chen, M. W. Wong, C. Gonzalez, J. A. Pople, Gaussian 03, Gaussian, Inc., Pittsburgh, PA (USA), **2003**.

Received: June 11, 2007
Published online: September 24, 2007